Weyl Semimetal in a Topological Insulator Multilayer

A. A. Burkov[1,2] and Leon Balents[2]

[1]Department of Physics and Astronomy, University of Waterloo, Waterloo, Ontario N2L 3G1, Canada
[2]Kavli Institute for Theoretical Physics, University of California, Santa Barbara, California 93106, USA

(Received 27 May 2011; published 16 September 2011)

We propose a simple realization of the three-dimensional (3D) Weyl semimetal phase, utilizing a multilayer structure, composed of identical thin films of a magnetically doped 3D topological insulator, separated by ordinary-insulator spacer layers. We show that the phase diagram of this system contains a Weyl semimetal phase of the simplest possible kind, with only two Dirac nodes of opposite chirality, separated in momentum space, in its band structure. This Weyl semimetal has a finite anomalous Hall conductivity and chiral edge states and occurs as an intermediate phase between an ordinary insulator and a 3D quantum anomalous Hall insulator. We find that the Weyl semimetal has a nonzero dc conductivity at zero temperature, but Drude weight vanishing as T^2, and is thus an unusual metallic phase, characterized by a finite anomalous Hall conductivity and topologically protected edge states.

DOI: 10.1103/PhysRevLett.107.127205 PACS numbers: 75.47.−m, 03.65.Vf, 71.90.+q, 73.43.−f

The recent discovery of time-reversal (TR) invariant topological insulators (TIs) [1] has led to a surge of interest in topological properties of the electronic band structure of crystalline materials. TIs exhibit a bulk gap but gapless surface states, whose gaplessness is protected by topology. Remarkably, recent work has demonstrated that such a surface-bulk correspondence can also be obtained even when the bulk is gapless, by virtue of point touchings of nondegenerate conduction and valence bands [2]. Such accidental point touchings have been known to exist since the earliest days of the theory of solids [3], but their topological properties have been appreciated only much more recently [2,4–6], and concrete materials, where they may be found, have been proposed [2,6]. Nontrivial and robust band touching requires either broken TR or inversion [2,3,5], in which case the touching points acquire topological character and thus give rise to stable phases of matter. The band structure near these points can be described by a massless two-component Dirac or Weyl Hamiltonian:

$$\mathcal{H} = \pm v_F \boldsymbol{\sigma} \cdot \mathbf{k}, \tag{1}$$

where $\mathbf{k}$ is the crystal momentum in the first Brillouin zone (BZ), expanded near the band-touching point, $\boldsymbol{\sigma}$ is the triplet of Pauli matrices, and the sign in front corresponds to two different possible chiralities, characterizing the point. Such Weyl fermions have been studied extensively in high-energy physics, in particular, as a description of neutrinos [4], and may be viewed as topological defects (hedgehogs) in momentum space [4]. Any perturbation of Eq. (1) only shifts the degeneracy point in energy or momentum but does not remove it: An isolated Weyl fermion in this sense possesses an absolute topological stability (this is in contrast to 2D massless Dirac fermions in graphene, where inversion symmetry of the honeycomb lattice is essential for their stability). Very general considerations show that Dirac degeneracy points can occur only in pairs of opposite chirality [7] and can thus be eliminated by pairwise annihilation. When the TR or inversion symmetry is broken, however, the Weyl fermions are separated in momentum space and thus, assuming translational symmetry remains intact, are still topologically stable.

Reference [2] has proposed a possible realization of a Weyl semimetal with 24 Dirac nodes in iridium pyrochlores, which are strongly correlated magnetic materials (a different scenario for this material was proposed in Ref. [8]). The purpose of this work is to propose a much simpler realization of the Weyl semimetal, not relying on strong correlations in a rather complex material. The Weyl semimetal we propose also possesses only two Dirac nodes, the smallest possible number, and thus is in a sense the most elemental realization of this phase of matter.

The material we propose is a multilayer heterostructure, consisting of alternating layers of a 3D TI material, such as Bi_2Se_3, and an ordinary insulator, which serves as spacer material between the neighboring TI layers, as shown in Fig. 1. The ability to grow ultrathin high-quality films of Bi_2Se_3 has been clearly demonstrated in recent experiments [9]. It is thus quite realistic to expect that a multilayer heterostructure, consisting essentially of a stack of such thin films, can be fabricated by using available technology. The Hamiltonian, describing this heterostructure, can be written as

$$H = \sum_{\mathbf{k}_\perp, ij} \Big[v_F \tau^z (\hat{z} \times \boldsymbol{\sigma}) \cdot \mathbf{k}_\perp \delta_{i,j} + m \sigma^z \delta_{i,j} + \Delta_S \tau^x \delta_{i,j} + \frac{1}{2} \Delta_D \tau^+ \delta_{j,i+1} + \frac{1}{2} \Delta_D \tau^- \delta_{j,i-1} \Big] c^\dagger_{\mathbf{k}_\perp i} c_{\mathbf{k}_\perp j}. \tag{2}$$

The first term in Eq. (2) describes the two (top and bottom) surface states of an individual TI layer. We assume for

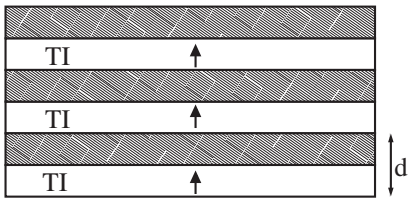

FIG. 1. Schematic drawing of the proposed multilayer structure. Unhashed layers are the TI layers, while hashed layers are the ordinary-insulator spacers. The arrow in each TI layer shows the magnetization direction. Only three periods of the superlattice are shown in the figure; 20–30 unit cells can perhaps be grown realistically.

simplicity that a TI material with a single two-dimensional (2D) Dirac node per surface BZ is employed. v_F is the Fermi velocity, characterizing the surface Dirac fermion, which we take to be the same on the top and bottom surface of each layer. $\mathbf{k}_\perp$ is the momentum in the 2D surface BZ (we use $\hbar = 1$ units), $\boldsymbol{\sigma}$ is the triplet of Pauli matrices acting on the real spin degree of freedom, and $\boldsymbol{\tau}$ are Pauli matrices acting on the surface pseudospin degree of freedom. The indices i and j label distinct TI layers. The second term describes exchange spin splitting of the surface states, which can be induced, for example, by doping each TI layer with magnetic impurities, as has been recently demonstrated experimentally [10]. The remaining terms in Eq. (2) describe tunneling between top and bottom surfaces within the same TI layer (the term proportional to Δ_S) and between top and bottom surfaces of neighboring TI layers (terms proportional to Δ_D). Longer-range tunneling is assumed to be negligible. We will regard m and $\Delta_{S,D}$ as tunable parameters and study the phase diagram of Eq. (2) as a function of these parameters.

Let us initially assume that the spin splitting is absent, i.e., set $m = 0$. Diagonalizing Eq. (2), one finds the following band dispersion:

$$\epsilon^2_{\mathbf{k}\pm} = v_F^2(k_x^2 + k_y^2) + \Delta^2(k_z), \tag{3}$$

where $\Delta(k_z) = \sqrt{\Delta_S^2 + \Delta_D^2 + 2\Delta_S\Delta_D \cos(k_z d)}$ and d is the superlattice period (i.e., the TI layer plus spacer layer thickness) in the growth (z) direction. This band structure is fully gapped when $|\Delta_S| \neq |\Delta_D|$ but contains Dirac nodes when $\Delta_S/\Delta_D = \pm 1$. The nodes are located at $k_z = \pi/d$ when $\Delta_S/\Delta_D = 1$ and at $k_z = 0$ when $\Delta_S/\Delta_D = -1$ ($k_x = k_y = 0$ always). While both cases are possible, we will assume the former for concreteness and will take both tunneling matrix elements to be positive (this choice does not affect any of our results). Expanding the band dispersion near the Dirac point at $k_x = k_y = 0$, $k_z = \pi/d$ to leading order in the momentum, one obtains

$$\epsilon^2_{\mathbf{k}\pm} = v_F^2(k_x^2 + k_y^2) + \tilde{v}_F^2 k_z^2, \tag{4}$$

where $\tilde{v}_F = d\sqrt{\Delta_S\Delta_D}$. The momentum-space Hamiltonian near the Dirac node has the form

$$\mathcal{H}(\mathbf{k}) = v_F\tau^z(\hat{z} \times \sigma) \cdot \mathbf{k} + \tilde{v}_F\tau^y k_z, \tag{5}$$

which can be brought to a block-diagonal form, explicitly revealing a pair of two-component Weyl fermions with opposite chirality, by a $\pi/2$ rotation around the x axis in the pseudospin space. Alternatively, in total this is a conventional four-component massless Dirac fermion. As discussed above, since the two Weyl fermions are located at the same point in momentum space, they are topologically unstable. Any perturbation, for example, any deviation of the ratio Δ_S/Δ_D from unity, immediately eliminates the degenerate Dirac node and produces a fully gapped spectrum. With $m = 0$, the massless Dirac point can be understood [5] as a critical point between topological ($\Delta_D > \Delta_S$) and ordinary ($\Delta_D < \Delta_S$) insulators with both inversion and time-reversal symmetry preserved [see Fig. 2(a)]. To produce a topologically stable phase with 3D Dirac nodes, the nodes have to be separated in momentum space. As mentioned above, this can generally be accomplished by breaking either TR or inversion symmetries, and there are in principle many ways to do this. Here we will focus on one particular way, which is perhaps the simplest from the point of view of a practical realization. Namely, as already mentioned above, we will assume that each TI layer is doped with magnetic impurities, producing a ferromagnetically ordered state within each layer, with magnetization along the growth direction of the heterostructure. This leads to spin splitting of the surface states of magnitude m, described by the second term in Eq. (2). The band dispersion is now given by

$$\epsilon^2_{\mathbf{k}\pm} = v_F^2(k_x^2 + k_y^2) + [m \pm \Delta(k_z)]^2. \tag{6}$$

This dispersion has two nondegenerate Dirac nodes, separated along the z axis in momentum space, with locations given by $k_z = \pi/d \pm k_0$, where

$$k_0 = \frac{1}{d}\arccos\{1 - [m^2 - (\Delta_S - \Delta_D)^2]/2\Delta_S\Delta_D\}. \tag{7}$$

The nodes exist as long as

$$m_{c1}^2 = (\Delta_S - \Delta_D)^2 < m^2 < m_{c2}^2 = (\Delta_S + \Delta_D)^2. \tag{8}$$

Thus, as discussed above, splitting of the degenerate Dirac node in momentum space produces a stable Weyl semimetal phase, existing in a finite region of the phase diagram [Fig. 2(b)]. The Weyl semimetal occurs as an intermediate phase between an ordinary insulator ($m^2 < m_{c1}^2$) and a 3D quantum anomalous Hall (QAH) insulator [11] with quantized Hall conductivity, equal to e^2/h per TI layer ($m^2 > m_{c2}^2$). As m is increased from zero, a degenerate Dirac point at $k_x = k_y = 0$, $k_z = \pi/d$ appears at the lower critical value (m_{c1}) of the spin splitting. The Dirac node is split along the z axis into two nondegenerate nodes in the Weyl semimetal phase, with the splitting increasing monotonically with the magnitude of m. At the upper

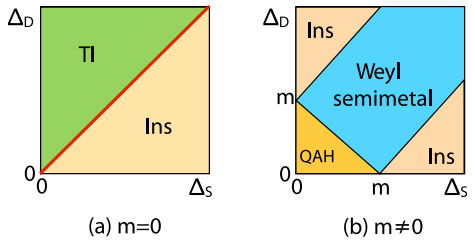

FIG. 2 (color online). Phase diagrams for (a) $m = 0$ and (b) $m \neq 0$. In (a), the red line represents the phase boundary between TI and ordinary insulator (Ins). In (b), due to TR symmetry breaking, the distinction between topological and ordinary insulators is moot, so the TI in (a) has been converted to Ins. QAH denotes the quantum anomalous Hall phase.

critical value (m_{c2}), the two nondegenerate nodes meet and annihilate at the center of the BZ $k_x = k_y = k_z = 0$, giving rise to the fully gapped QAH insulator.

We will now show that the Weyl semimetal phase we have found is characterized by a nonzero, but nonquantized, anomalous Hall conductivity, proportional to the magnitude of the separation of the Dirac nodes in momentum space, thus smoothly evolving from zero in the ordinary-insulator phase to e^2/h per layer in the 3D QAH insulator phase.

The fact that a 3D Weyl semimetal generally has a finite Hall conductivity is known and was pointed out, e.g., in Ref. [12]. For the particular realization of a Weyl semimetal, proposed in Ref. [2], the Hall conductivity vanishes due to the cubic symmetry of the crystal structure of the pyrochlore iridate materials. If the cubic symmetry is broken, e.g., by applying a uniaxial pressure, as proposed in Ref. [6], the Hall conductivity becomes nonzero and is proportional, in the case discussed in Ref. [6], to the applied pressure. In our case, there is a natural preferred axis; i.e., the growth direction of the heterostructure (which coincides with the magnetization direction) and the Hall conductivity in the Weyl semimetal phase is automatically nonzero. The simplest and most physically transparent way to obtain this result is to view the 3D band structure as a set of independent 2D band structures at fixed k_z. We begin with the momentum-space Hamiltonian:

$$\mathcal{H}(\mathbf{k}) = v_F \tau^z (\hat{z} \times \boldsymbol{\sigma}) \cdot \mathbf{k} + m\sigma^z + \hat{\Delta}(k_z), \qquad (9)$$

where $\hat{\Delta} = \Delta_S \tau^x + \frac{1}{2}(\Delta_D \tau^+ e^{ik_z d} + \text{H.c.})$. This is simplified by the canonical transformation:

$$\sigma^\pm \rightarrow \tau^z \sigma^\pm, \qquad \tau^\pm \rightarrow \sigma^z \tau^\pm. \qquad (10)$$

After this transformation, the Hamiltonian becomes

$$\mathcal{H}(\mathbf{k}) = v_F k_y \sigma^x - v_F k_x \sigma^y + [m + \hat{\Delta}(k_z)]\sigma^z. \qquad (11)$$

Now $\hat{\Delta}$ is a constant of motion and may be replaced by its eigenvalues $\hat{\Delta}(k_z) = \pm\Delta(k_z)$. For each of these cases, Eq. (11) gives a 2D Dirac Hamiltonian for fixed k_z, with a mass $M_\pm = m \pm \Delta(k_z)$. For $m > m_{c1}$, M_- vanishes when $k_z = \pi/d \pm k_0$, corresponding to the two Dirac nodes (M_+ never vanishes).

It is well known that a change of sign of a 2D Dirac mass signals a quantum Hall transition, at which the quantized 2D Hall conductivity σ_{xy}^{2D} jumps by e^2/h [13]. The absolute value of the Hall conductance is not determined by the above continuum model. Therefore the contribution to the total 3D Hall conductance of the states at fixed k_z is equal to $\sigma_{xy}^{2D}(k_z) = e^2/h[n + \Theta(k_0 - |k_z - \pi/d|)]$, where $\Theta(x)$ is the Heaviside step function and n is an integer. Since when m vanishes TR symmetry demands that the Hall conductivity must also vanish, we can conclude that $n = 0$, and hence

$$\sigma_{xy} = \int_{-\pi/d}^{\pi/d} \frac{dk_z}{2\pi} \sigma_{xy}^{2D}(k_z) = \frac{e^2 k_0}{\pi h}. \qquad (12)$$

Thus the anomalous Hall conductivity in the Weyl semimetal is proportional to the separation of the Dirac nodes in momentum space. For a multilayer, consisting of a finite number of layers, as will be the case in the experiment, σ_{xy} will exhibit plateaus as a function of m, when k_0 will fall in an interval between the neighboring quantized k_z values, as shown in Fig. 3. At the upper critical value of $m = m_{c2}$, $2k_0 = 2\pi/d$, the two Dirac nodes annihilate each other at the center of the BZ, and the Hall conductivity reaches a quantized value per TI layer:

$$\sigma_{xy} = \frac{e^2}{dh}, \qquad (13)$$

which characterizes the $m > m_{c2}$ 3D QAH insulator phase.

The results of Ref. [2] imply the existence of ''Fermi arcs'' for the Weyl semimetal, in this case for any surface except the one normal to the z axis. In fact, this arc is nothing but the set of edge states corresponding to the 2D integer quantum Hall states for $\pi/d - k_0 < |k_z| < \pi/d$. These can be explicitly found from Eq. (11) for, e.g., the case of a surface at $y = 0$, modeled by a y-dependent spin-splitting field $m(y)$. Outside the sample ($y > 0$) we take $m(y \rightarrow +\infty) = 0$, which realizes an ordinary insulator, while $m > m_{c1}$ for $y < 0$, and consider the eigenstates for fixed k_x and k_z. There are then special surface wave functions with $\hat{\Delta}(k_z) = -\Delta(k_z)$, which are eigenstates of (11):

$$\psi_{\text{surf}}(k_x, k_z; y) = e^{\int_0^y dy'[m(y') - \Delta(k_z)]/v_F} |\sigma^y = -1\rangle. \qquad (14)$$

For $\pi/d - k_0 < |k_z| < \pi/d$ and not otherwise, the exponential above vanishes when $y \rightarrow \pm\infty$ and the state is normalizable and localized to the surface with a localization length $\xi(k_z) \sim v_F/M_-(k_z)$. The energy of this state is simply $\epsilon_{\text{surf}} = v_F k_x$, indeed identifying it as a chiral edge state. As m is increased to enter the QAH insulator phase, the arc extends across the full BZ and then the surface states can be alternatively viewed in a Wannier basis

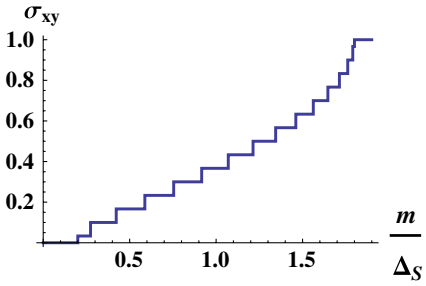

FIG. 3 (color online). A plot of σ_{xy} in units of e^2/hd for a multilayer consisting of 30 TI layers. Δ_D is taken to be equal to $0.8\Delta_S$. The Hall conductivity is zero in the ordinary-insulator phase ($m < \Delta_S - \Delta_D$) and reaches the maximum value of e^2/hd in the QAH phase ($m > \Delta_S + \Delta_D$). Plateaus correspond to the wave vector k_0 being in an interval between the neighboring finite-size-quantized k_z values.

localized in individual TI layers, i.e., as conventional quantum Hall edge states for each layer.

While the Weyl semimetal has topologically protected edge states (topological protection follows from the separation of the Dirac nodes in momentum space and from the fact the edge states are chiral), it is actually not a Hall insulator. At first sight, the low density of states $g(\epsilon) \sim \epsilon^2$ seems to suggest a vanishing dc conductivity at zero temperature [2]. However, a careful calculation reveals that, in the presence of disorder but not interactions, this is not the case. By using the standard Kubo formula expression (or Boltzmann equation) with the Born-approximation impurity scattering rate $1/\tau(\epsilon) = 2\pi\gamma g(\epsilon)$, where $g(\epsilon) = \epsilon^2/2\pi^2 v_F^3$ and γ characterizes the strength of the impurity potential, the optical conductivity of a Weyl semimetal with isotropic Fermi velocity v_F at temperature T is given by

$$\mathrm{Re}\,\sigma(\omega) \sim \frac{e^2 v_F^2}{h\gamma} \int_{-\infty}^{\infty} dx \frac{x^4 \mathrm{sech}^2(x)}{x^4 + (h^3 v_F^3 \omega/32\pi^2\gamma T^2)^2}, \quad (15)$$

where we have restored explicit $\hbar$ for clarity. This gives a finite dc conductivity $\sigma_{\mathrm{DC}} \sim e^2 v_F^2/h\gamma$, which can be expected to be large in a clean multilayer, but a Drude-like peak in the optical conductivity with weight, vanishing as T^2. Thus with disorder (but neglecting interactions), the Weyl semimetal is not an insulator but an unusual metal, characterized by a nonzero anomalous Hall conductivity and topologically protected edge states.

In conclusion, we have proposed a simple realization of a 3D Weyl semimetal phase in a multilayer structure, composed of a stack of thin layers of magnetically doped 3D TI material, separated by insulating spacers. We have shown that this material realizes the simplest possible type of Weyl semimetal, with only two Dirac nodes, separated along the growth direction of the heterostructure in momentum space. This Weyl semimetal is characterized by a nonzero anomalous Hall conductivity, proportional to the separation between the Dirac nodes, and by the existence of topologically stable chiral edge states. These edge states are, however, distinct from the ordinary quantum Hall edge states, since they exist not in the whole edge BZ but in its finite subset, whose size is determined by the momentum-space separation of the Dirac nodes. Finally, we find that the Weyl semimetal has a finite dc conductivity at zero temperature, but Drude weight vanishing as T^2, and is thus an interesting metallic state, characterized by a nonzero anomalous Hall conductivity and topologically protected edge states. Interesting open questions include the influence of Coulomb interactions on the properties of Weyl semimetals, in particular, their transport properties.

We acknowledge useful discussions with Matthew P. A. Fisher, Ying Ran, and Cenke Xu. Financial support was provided by the NSERC of Canada and a University of Waterloo start-up grant (A. A. B.), by NSF Grants No. DMR-0804564 and No. PHY05-51164 (L. B.), and by the Army Research Office through MURI Grant No. W911-NF-09-1-0398 (L. B.). A. A. B. gratefully acknowledges the hospitality of KITP, where this work was done.

[1] C. L. Kane and E. J. Mele, Phys. Rev. Lett. **95**, 146802 (2005); B. A. Bernevig, T. L. Hughes, and S.-C. Zhang, Science **314**, 1757 (2006); J. E. Moore and L. Balents, Phys. Rev. B **75**, 121306 (2007); L. Fu, C. L. Kane, and E. J. Mele, Phys. Rev. Lett. **98**, 106803 (2007); Y. Xia *et al.*, Nature Phys. **5**, 398 (2009); M. Z. Hasan and C. L. Kane, Rev. Mod. Phys. **82**, 3045 (2010); X.-L. Qi and S.-C. Zhang, arXiv:1008.2026 [Rev. Mod. Phys. (to be published)].
[2] X. Wan *et al.*, Phys. Rev. B **83**, 205101 (2011).
[3] C. Herring, Phys. Rev. **52**, 365 (1937).
[4] G. E. Volovik, *The Universe in a Helium Droplet* (Clarendon, Oxford, 2003); Lect. Notes Phys. **718**, 31 (2007).
[5] S. Murakami, New J. Phys. **9**, 356 (2007).
[6] K.-Y. Yang, Y.-M. Lu, and Y. Ran, Phys. Rev. B **84**, 075129 (2011).
[7] H. B. Nielsen and N. Ninomiya, Nucl. Phys. **B185**, 20 (1981); **B193**, 173 (1981).
[8] D. A. Pesin and L. Balents, Nature Phys. **6**, 376 (2010).
[9] G. Zhang *et al.*, Appl. Phys. Lett. **95**, 053114 (2009); H. Peng *et al.*, Nature Mater. **9**, 225 (2010); Y. Zhang *et al.*, Nature Phys. **6**, 584 (2010).
[10] Y. L. Chen *et al.*, Science **329**, 659 (2010).
[11] R. Yu *et al.*, Science **329**, 61 (2010).
[12] F. R. Klinkhamer and G. E. Volovik, Int. J. Mod. Phys. A **20**, 2795 (2005).
[13] A. W. W. Ludwig *et al.*, Phys. Rev. B **50**, 7526 (1994).